IAC-10.A6.1.9

# ANALYSIS OF OBSERVED AND SIMULATED LIGHT CURVES OF SPACE DEBRIS

**Carolin Früh**
Astronomical Institute, University of Bern, Switzerland
frueh@aiub.unibe.ch

Thomas Schildknecht[1]

Since 2004, the Astronomical Institute of the University of Bern (AIUB) has regularly observed light curves of fast-moving Earth-orbiting objects with the 1-meter telescope ZIMLAT, which is located near Bern, Switzerland. A light curve represents the brightness variations of an object over time. These variations result from the superposition of shape, attitude, motion, and material of an object under a specific viewing and illumination geometry. Whereas actively stabilized objects show relatively flat light curves due to stable attitude, light curves of space debris can show large variations even within very short time intervals. The time resolution of the light curves acquired with ZIMLAT is of the order of a few seconds, but even this high resolution does not prevent aliasing effects in some cases. Synthetic light curves have been generated. The simulation allows defining and independently changing object, illumination, and observation geometry parameters. This paper analyzes observed and simulated light curves with the aim to assess the feasibility of determining an object's characteristics, provided that the observation parameters (epoch, orbit/distance and geometry) are known.

## I. Introduction

Since the first satellite, Sputnik, was launched, more and more resident space objects (RSOs) are populating the space around the Earth. The USSTRATCOM catalog counts around 16 000 objects. Estimates by other sources, such as the Astronomical Institute of the University of Bern, assume more than 300 000 objects larger than one centimeter orbiting the Earth. As the numbers indicate, only a small portion of the objects are actually known. With the increasing number of unknown resident space objects, it becomes more and more challenging to distinguish objects from each other and uniquely identify them. The images of objects at an altitude of 36000 km in the geostationary ring are non-resolved in ground-based observations. One way to gain more than positional information is through light curve measurements. Light curves measure the light reflected from an object over time in a specific viewing direction. The reflected light is a super-position of the shape and attitude motion of an object under a specific viewing geometry. The Astronomical Institute of the University of Bern measures light curves of RSOs – active spacecraft and space debris – on a regular basis since 2004. This paper addresses the issue of analyzing the measured light curves of space debris. For a deeper insight, artificial light curves of simple shapes are simulated. In simulated light curves, all parameters, such as shape, attitude, lighting, and viewing conditions are known and can

[1]Astronomical Institute, University of Bern, Switzerland, thomas.schildknecht@aiub.unibe.ch

be controlled. They serve as test cases and a learning environment for real light curves. Possible analogies between simulated and measured light curves are investigated.

This paper is giving a very brief introduction to the theory of light curve measurements. In the following section, the mechanism of simulating light curves and some examples are shown. This section is followed by examples of measured light curves of an active satellite and space debris. The light curves are Fourier analyzed and a pattern recognition method is introduced. The conclusions summarize the results.

## II. Theory of Light Curve Observations

In light curve measurements, the brightness of a non-resolved object is measured over time, observed in a specific viewing direction. The light received by the observer depends on the geometry under which the object is observed, the materials the object is composed of, the orientation of all illuminated facets, the illumination, and the observation direction. An example of a possible viewing geometry is shown in Fig. 1. A local coordinate system of the RSO is defined, along its main axis of inertia. The classical phase angle, Earth-object-Sun, is split into two angles, in the xy-plane and in the xz-plane.

The radiant intensity reaching the Earth is therefore:

$$I = \frac{I_{sun} A_{eff}}{4\pi R^2_{earth-obj}} \qquad (1)$$

with:

$$A_{eff} = \Sigma_{j=1}^{N_{facets}} A_j a_j (\vec{n}_j \vec{i})_+ (\vec{n}_j \vec{o})_+ \qquad (2)$$

$I_{sun}$ is the Sun's radiation intensity at the object, $R_{earth-obj}$ the distance between observer and object, and $A_{eff}$ the effective surface. The effective surface is a sum over all illuminated $(\vec{n}_j \vec{i}_j)_+$ and visible $(\vec{n}_j \vec{o})_+$ facets with their individual albedos $a_j$, whereas $\vec{n}$ is the normal vector on each facet, $\vec{i}$ is the light vector object-Sun, and $\vec{o}$ the vector object-observer. The +-subscript indicates that only positive values are taken into account.

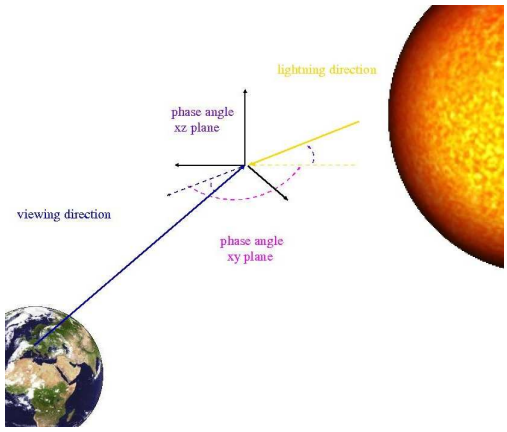


Figure 1: Lighting and viewing conditions in observing an Earth orbiting RSO.

## III. Simulated Light Curves

To analyze light curves, two independent approaches have been taken. First, light curves of simple shapes have been simulated. The shapes were rendered and animated with OpenSceneGraph under different lighting and viewing geometries. The light source was calibrated to represent a realistic lighting from the Sun. The illuminated and visible facets were integrated at discrete time steps. With calibration and assumption of the size and distance of the simulated objects, magnitudes can be estimated. A cube, a cylinder, and the shape of a thin multi-layer insulation (MLI) structure have been simulated. For all simulations shown in this paper, all shapes are assumed to be pure Lambertian reflectors. Spectral reflection has been simulated, too. Pure spectral reflectors produce specific glint patterns with times of invisibility in between. The cube was simulated to have a sides of two meters, the cylinder was simulated to have a height of 6.2 meters and a diameter of 3.7 meters, which represents the size of an average Russian upper stage, and the MLI structure was assumed to have a size of roughly one

square meter. All objects are assumed to be in the geostationary ring with zero inclination. Without loss of generality the observer was assumed to be in the same plane as the object.

For the cylinder, four different setups are displayed. First, a single rotation around the x-axis in the coordinate system of the cylinder, with a period of 41 minutes under a phase angle of zero degrees, is simulated. Second, two rotations which superimpose on each other, one around the x-axis with a period of 49 minutes and one around the y-axis with a period of 88 minutes, is examined. This latter rotation was simulated to be observed under a phase angle of 0 degrees, of 90 degrees in the xy-plane, and under 90 degrees in xy-plane and 45 degrees in the xz-plane. The time scale used is arbitrary – it was assumed that every time step rendered corresponds to a sampling of one second. This choice makes the simulation independent of the specific platform it is run on. Fig. 2 illustrates the cylinder in the different lighting/viewing conditions and Fig. 3 displays the different synthetic light curves gained in the different setups. The latter setup of an illumination from a source 90 degrees in plane and 45 degrees out of plane seen from the observer, and the superimposed rotation of 49 resp. 88 minutes around the x- and y-axis was also simulated for the cube and the MLI structure, both as pure Lambertian reflectors again. In Fig. 4 and Fig. 5, the shapes and setup, as well as the light curves, are shown.

Fig. 3 shows that the simple rotation around the x-axis only and the rotation around two axis (x- and y-axis) do not produce completely different patterns – mostly the time scale seems to differ – as long as the phase angle is zero in the xy-, as well as in the xz-plane. The very same rotation produces different patterns, when the phase angles are changed, due to the fact that not all facets that are illuminated are visible to the observer.

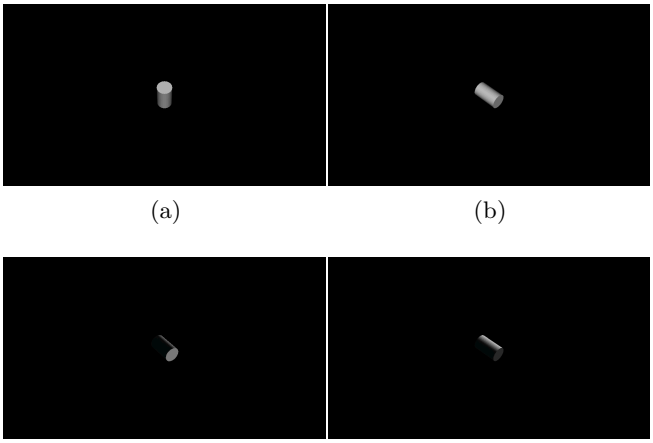

(a) (b)

(c) (d)

Figure 2: Simulated cylinder under different lighting and rotation conditions: (a) rotation around x-axis, phase angle 0°. Rotation around x- and y-axis with frequencies 5:3, with phase angle (b) 0°, (c) 90° in xy-plane, and (d) 90° in xy-plane and 45° in xz-plane

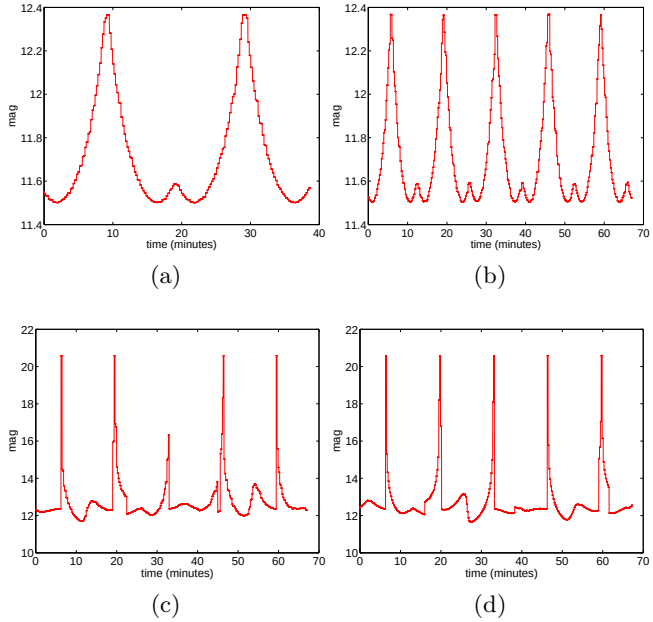


(a) (b)

(c) (d)

Figure 3: Simulated light curves of a cylinder under different lighting and rotation conditions: (a) rotation around x-axis (41min period), phase angle 0°. Rotation around x- and y-axis (period 49 resp. 88min), with phase angle (b) 0°, (c) 90° in xy-plane, and (d) 90° in xy-plane and 45° in xz-plane

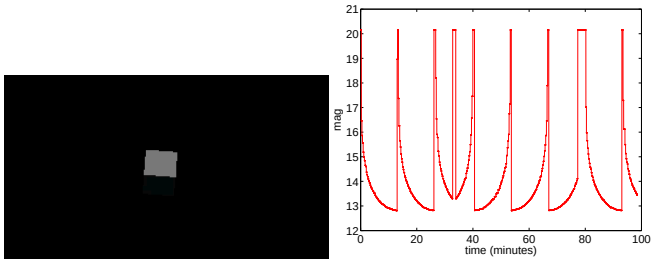


(a) (b)

Figure 4: Simulation of a cube with rotation around x- and y-axis (period 49 resp. 88min), with phase angle 90° in xy-plane and 45° in xz-plane: (a) image of the simulation, and (b) simulated light curve.

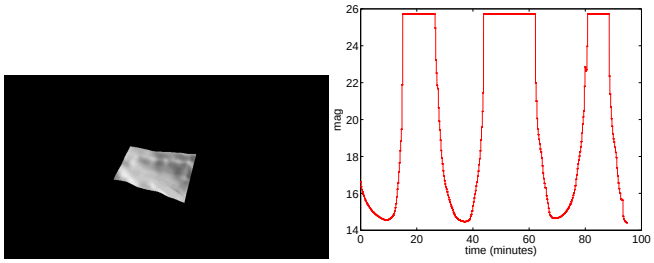


(a) (b)

Figure 5: Simulation of an MLI structure with rotation around x- and y-axis (period 49 resp. 88min), with phase angle 90° in xy-plane and 45° in xz-plane: (a) image of the simulation and (b) simulated light curve.

In a comparison of Fig. 3 with Fig. 4 and Fig. 5, the simulations of the cube and the MLI structure show that the light curves also differ for the very same setup if the viewing geometry and lighting conditions for different shapes differ significantly. If the object consist of one or only a few flat surfaces, and it is in a tulbing motion, it is not visible for the observer during the observation span several times.

## IV. Observed Light Curves

With the 1-meter ZIMmerwald Laser and Astrometric Telescope (ZIMLAT), light curves of space debris are observed on a regular basis. Most of the light curves are collected from space debris objects that are not in the official USSTRATCOM catalog, but are maintained in the internal AIUB catalog. A small subset of three objects from the USSTRATCOM catalog was chosen, to be displayed here. If the objects are known, i.e, are in the USSTRATCOM catalog, the objects are already identified, thus the shape of the objects is known. Characterization of known objects is one simplification on the way to a full characterization of completely unknown objects. The sampling rate of light curves taken with ZIMLAT is of the order of three seconds.

First, light curves of the spin controlled MSG-1 satellite with the COSPAR Number 2002-040B were taken. MSG-1 is a cylindrically shaped satellite, which is still active and has a spin-stabilized attitude control.

As a second case, the Blok DM-2 upper stage 1991-010F was observed. The upper stage is shaped more or less cylindrically; it was never in a controlled attitude state.

Third, the dead Gorizont 33 satellite 1990-102A was observed and light curves were taken. The Gorizont satellite consists very basically of a cylindrically shaped body with two larger and two smaller solar panels. It is space debris and no longer attitude controlled.

All objects are in a geostationary orbit, with negligible eccentricities. MSG-1 is in a controlled orbit around zero degrees inclination, Blok DM-2 is in an orbit with an inclination of 11.9 degrees, and the Gorizont 33 satellite at 12.5 degrees inclination.

Two light curves of MSG-1 are displayed, taken on Dec 4th under a phase angle of 40.2° and on Dec 9th under 93°; the light curves are displayed in Fig. 6. For Blok DM-2, four light curves are analyzed, observed on May 12th, 13th, 19th, and 26th, under phase angles of 21.1°, 9.5°, 14.9° and 31.4°, respectively, displayed in Fig. 7. Three light curves of Gorizont 33 are examined, taken on July 21st

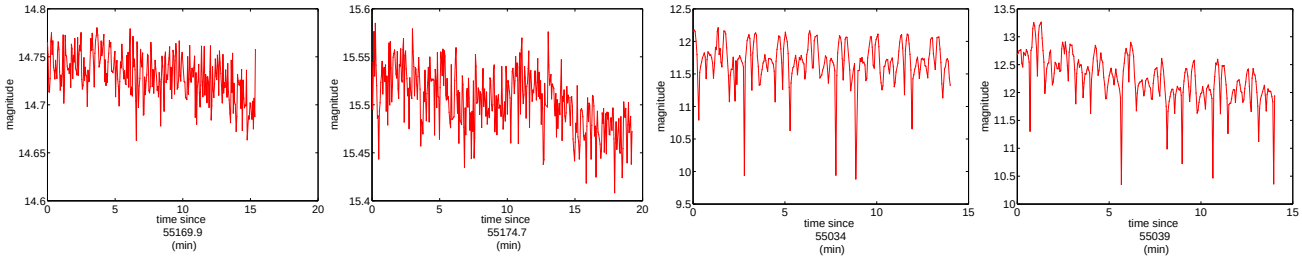


(a) (b) (a) (b)

Figure 6: Light curves of the MSG-1 satellite 2002-040B (a) Dec 4th, phase angle 42.2° and (b) Dec 9th, phase angle 93°.

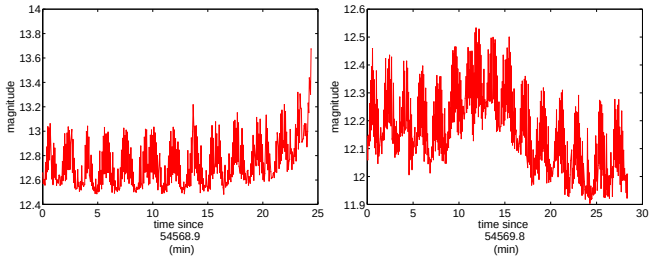


(a) (b)

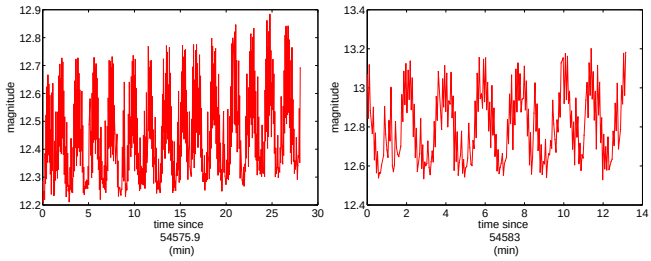


(c) (d)

Figure 7: Light curves of the Blok DM-2 satellite 1991-010F (a) May 12th, phase angle 21.1°, (b) May 13th, phase angle 9.5°, (c) May 19th, phase angle 14.9°, and (d) May 26th, phase angle 31.4°.

at a phase angle of 11.4°, July 26th and July 28th, under an angle of 11.2° resp. 15.1°; they are displayed in Fig. 8.

All magnitudes that are displayed are apparent magnitudes, calibrated against the stellar background. The measurements were taken over time intervals up to 30 minutes.

In Fig. 6, the two light curves of the spin-stabilized satellite MSG-1 satellite are very

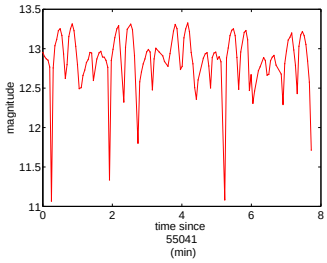


(c)

Figure 8: Light curves of the Gorizont 33 satellite 1990-102A (a) July 21st, phase angle 11.4°, (b) July 26th, phase angle 11.2°, and (c) July 28th, phase angle 15.1°.

flat and only show small fluctuations within the limits of about 0.1 apparent magnitudes over the observation interval. This is expected, due to the controlled attitude state and the cylindrical shape. The only rotation that is performed is around the symmetry axis of the cylinder, which is expected to be vertical to the observation direction. That small fluctuations are observed can have two possible explanations. For one, the surface of the MSG-1 cylinder is not completely uniform, it consists of several flat surfaces of the panels and other smaller substructures. Furthermore, of course, fluctuations in the atmosphere is a major uncertainty factor, too.

In Fig. 7, the light curves of Blok DM-2 are displayed. They show clear structures and variations of the order of half a magnitude within few seconds. The light curves vary from one observation to the next. The very fast variations suggest that aliasing effects may be present.

Fig. 8 shows three light curves of the Gorizont satellite. For this large satellite, there seems to be a pattern present in each of the observations, suspected to represent the panel-body structure. The light curves are not identical, even when observed under very similar phase angles as in Fig. 8 (a) and (b), but resemble each other strongly.

## V. Fourier Analysis

To gain more insight, the light curves were Fourier analyzed. In the first step, the simulated light curves were analyzed. The results for the cylinder are shown in Fig. 9. Fig. 9(a) shows the Fourier spectrum for the simple x-axis rotation. There, one main period shows up prominently. But its value is of about eight minutes and additionally several smaller periods show up. Eight minutes is much smaller than the true period that was used to generate the synthetic light curve. One reason is, that compared to the period only a short observation interval of 40 minutes was assumed, which may very well be a realistic scenario, but it cannot be expected that the Fourier decomposition actually produces the correct period under these circumstances. As a second test, a longer observation interval of 200 minutes was assumed of the very same setup. A Fourier analysis was performed. The light curve itself and the Fourier decomposition is shown in Fig. 10. The Fourier decomposition has changed significantly. There is one main period at 20 minutes and one at around 10 minutes. The period of 20 minutes is actually close to half of the actual rotation period, which is due to the fact that the cylinder is mirror symmetric to the xy-plane.

Fig. 9(a) to (c) show the Fourier spectrum for the light curves of the superimposed rotation around the x- and the y- axis. All light curves show two main periods of around six and eleven minutes. The cases observed under a phase angle different from zero also show several other distinct periods but with smaller amplitudes especially in the cases. The are indeed two main rotations – the introduced rotation rates were 88 and 49 minutes – but the assumed observation interval is again far too short to catch these periods in the Fourier analysis. What is preserved nevertheless is the relation of about 1.8 between the periods.

Fig. 11 shows the Fourier decomposition for the simulated cube and the MLI structure for the same rotation as the latter case of the cylinder. The cube (Fig. 11(a)) shows two main periods, one at around 6 minutes and another one at around 12 minutes, consisting of two not clearly separated periods. The result is, therefore, comparable to the case of the same setup for a cylinder. The situation is different for the MLI structure, (Fig. 11(b)). Here, the Fourier analysis shows one main dominant period at 23 minutes, and smaller ones at about 12 and 16 minutes. Obviously, with the large periods in which the object is not visible for the observer due to the flat shape, the Fourier decomposition of the different rotations is complicated.

In the next step, the real light curves were Fourier analyzed. Fig. 12, the Fourier analysis of the controlled MSG-1 satellite, shows no large amplitudes for any periods. This is in accordance with what one expects for a spin-stabilized satellite. Fig. 13 shows the Fourier spectrum for the Blok DM-2 light curves displayed in Fig. 7. For all four light curves, one very small period of the order of 4 to 8 seconds occurs with a large amplitude, as well as one or two not clearly separated periods around 1.3 to 1.8 minutes. This strongly indicates that the observed light curves are subject to aliasing effects, due to a 3-second sampling rate. The main periods seem to be more or less stable over the different phase angle measurements and times. But Fig. 7(b) especially seems to indicate that there may be at least one large period superimposed, which cannot be detected with the current length of the observation interval in a Fourier analysis.

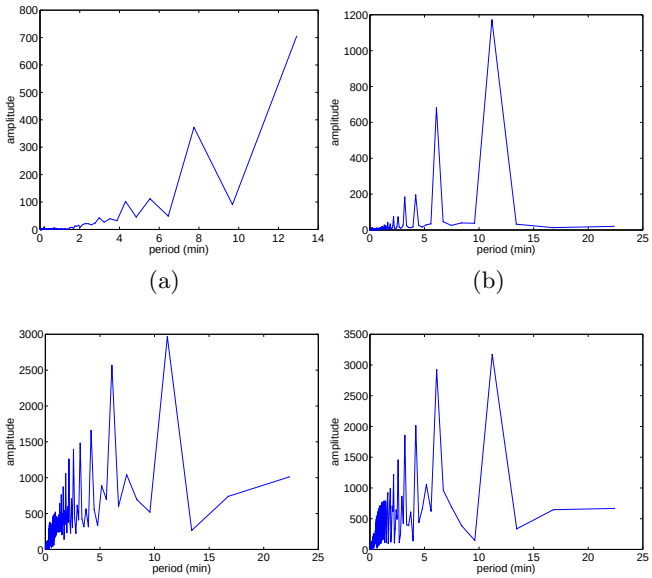


Figure 9: Fourier spectrum of simulated light curves of a cylinder under different lighting and rotation conditions: (a) rotation around x-axis (41-min period), phase angle 0°. Rotation around x- and y-axis (period 49 resp. 88min), with phase angle (b) 0°, (c) 90° in xy-plane, and (d) 90° in xy-plane and 45° in xz-plane.

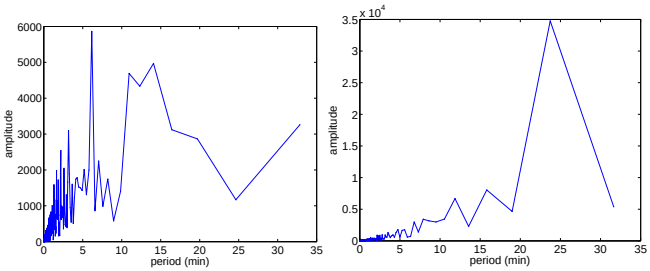


Figure 11: Fourier spectrum of the simulated light curves of (a) a cube and (b) MLI structure with rotation around x- and y-axis (period 49 resp. 88min), with phase angle 90° in xy-plane and 45° in xz-plane.

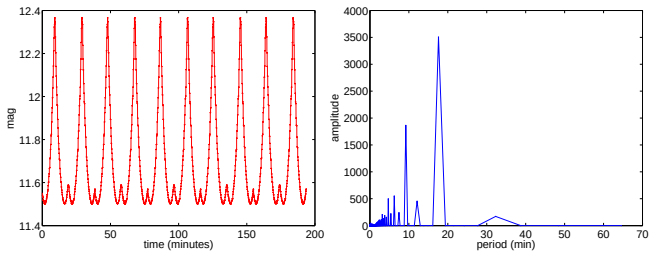


Figure 10: (a) Simulated light curves over a long observation interval for a cylinder rotating with a period of 41 minutes around x-axis, phase angle 0°; (b) Fourier spectrum of this light curve.

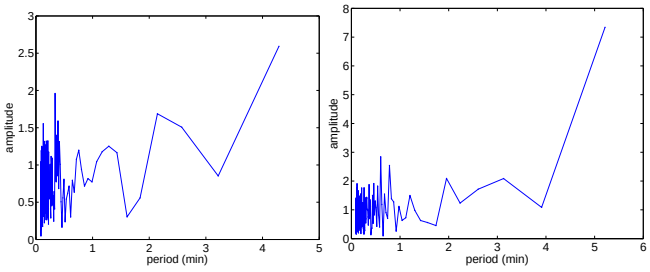


Figure 12: Fourier spectrum of light curves of the MSG-1 satellite 2002-040B (a) Dec 4th, phase angle 42.2° and (b) Dec 9th, phase angle 93°.

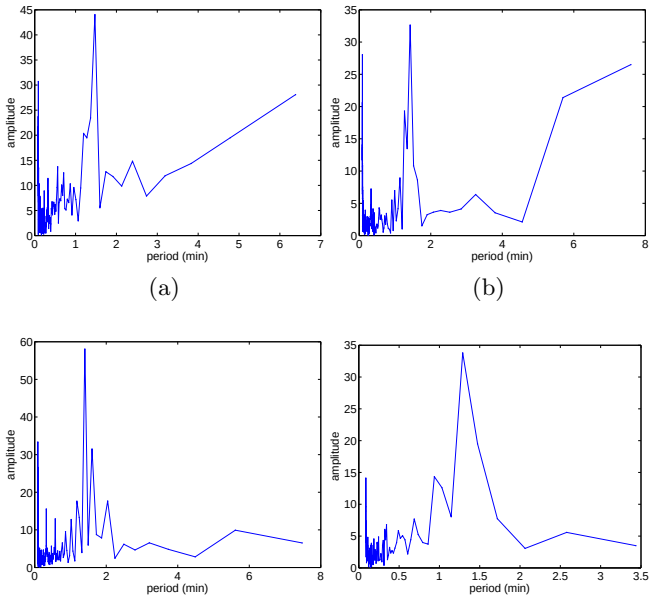


Figure 13: Fourier spectrum of light curves of the Blok DM-2 satellite 1991-010F (a) May 12th, phase angle 21.1°, (b) May 13th, phase angle 9.5°, (c) May 19th, phase angle 14.9°, and (d) May 26th, phase angle 31.4°.

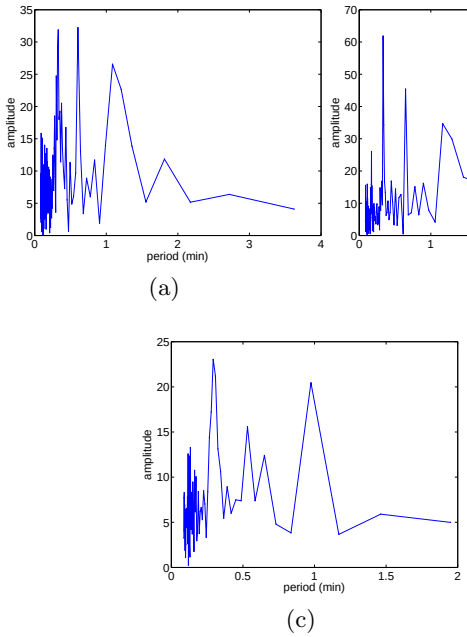


Figure 14: Fourier spectrum of light curves of the Gorizont 33 satellite 1990-102A (a) July 21st, phase angle 11.4°, (b) July 26th, phase angle 11.2°, and (c) July 28th, phase angle 15.1°.

The Fourier analysis of the three light curves of Gorizont 33 (Fig. 8) are displayed in Fig. 14. They show three main periods around 25 and 35 seconds and one around one minute. In Fig. 14(c) the second period is split into two periods, which are not completely separated.

Although the observation intervals are short, this indicates very rapid rotations for the debris objects. The difference between sidereal and synodal rotation is not relevant for geostationary objects observed over short time intervals of the order of less then 1/24 of their revolution period. The periods seem to be more or less constant for observations under different phase angles.

## VI. Pattern Analysis

In a next step, a pattern recognition algorithm was developed. The algorithm tries to detect pattern in light curves measurements. A pattern is a set of data points which is within small deviations re-detected within the same light curve several times.

The algorithm was tested with the simulated light curve of a cylinder rotation around the x-axis observed under phase angle zero, which is displayed in Fig. 3(a). The results are shown in Fig. 15: Fig. 15(a) shows the size of the patterns found as a function of the number of times the pattern could be

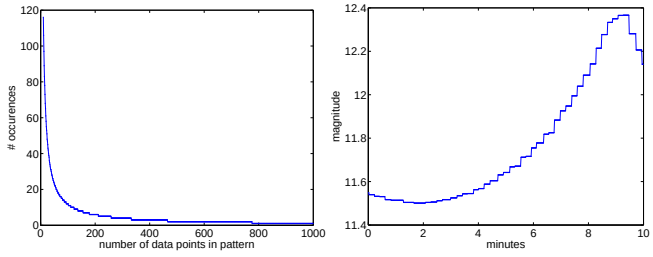


Figure 15: (a) Size of the pattern as a function of the number of detected occurrences (b) pattern found in light curve of Fig. 3(a).

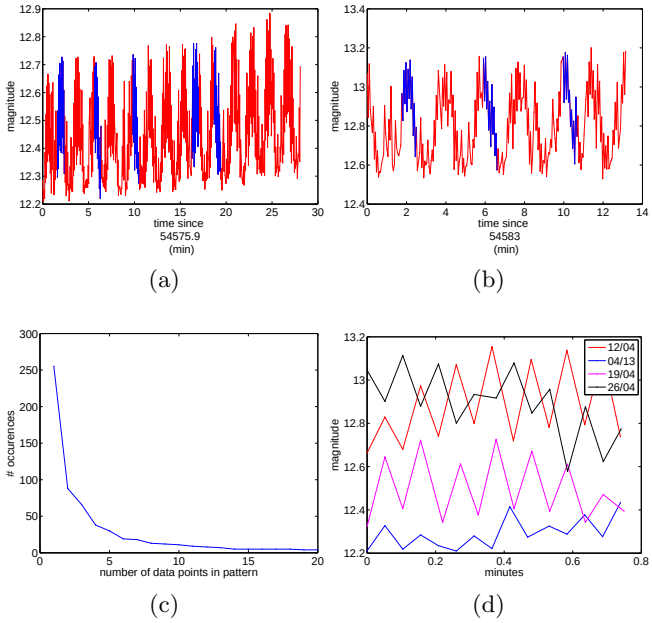


Figure 16: Light curves with highlighted pattern of the Blok DM-2 satellite 1991-010F (a) May 19th and (b) May 26th. In (c), the size of the pattern as a function of the number of detected occurrences in the light curve of May 19th. (d) Patterns found in all four light curves of Fig. 7 in one plot.

found again within the same light curves up to small deviations of 20 percent. Fig. 15(b) shows the pattern that was found. The pattern is probably slightly shifted compared to one chosen by eyesight, but the algorithm was judged to be working. The selected pattern was programmed to be chosen as large as possible, a size of 600 data points still occurs three times, which seemed to be a reasonable value with regard to number of data points (about 2,400). At this step, the algorithm still relies on some experience values.

In the second step, the real light curves were analyzed. In all cases, patterns could be found. Fig. 16(a) and (b) show two of the light curves of Blok DM-2; the detected patterns are highlighted. The size of the pattern as a function of the number of detections are displayed in Fig. 7(c), exemplary for the light curve measured on May 19th. The detected patterns of all four light curve of Blok DM-2

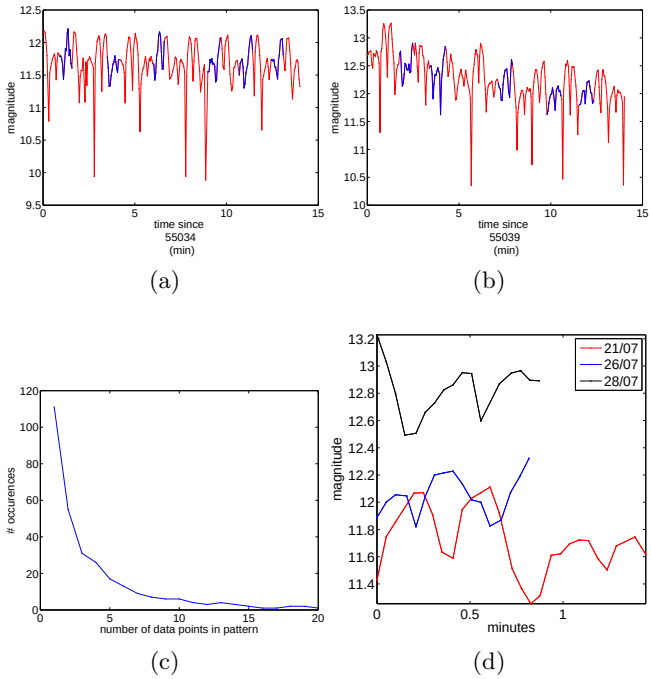


Figure 17: Light curves with highlighted pattern of the Gorizont 33 satellite 1990-102A (a) July 21st and (b) July 26th. In (c), the size of the pattern as a function of the number of detected occurrences in the light curve of July 21st. (d) Patterns found in all three light curves of Fig. 8 in one plot.

are shown in Fig. 7. It was possible to detect patterns in all four light curves, the size of the pattern cover 16 to 17 data points of a total of the order of 350 to 500 data points the light covers consist of. The patterns are not identical for all four light curves – the magnitudes are not the same – which might be due to observations under different phase angles. The pattern is not found as often as a check by eye would suggest, compared to Fig. 7(a) and Fig. 7(b). That was due to the fact, that the allowed deviations would have to be enlarged to count more occurrences, but this also leads to obvious mistagging.

Fig. 17 shows two of the light curves with highlighted patterns of Gorizont 33 and the dependence of the pattern size of the number of detected occurrences. The size of the patterns that could be detected in all light curves cover 16 to 27 data points. Although, here again, the single patterns that could be found are not identical, they clearly show a different structure than for the upper stage Blok DM-2, compared to Fig. 16(d) and Fig. 17(d). In both cases, it has to be stated that the periods found in the Fourier analysis are of the order of the successful pattern detected in the light curves.

## VII. Conclusions

Light curves of simple shapes under different lighting, viewing conditions, and rotation states have been simulated. The experience gained there was used to be able to better appraise the real light curve measurements and their analysis.

All light curves, synthetic and observed, were Fourier analyzed. The simulated light curves showed that for the cylindrical shape and the cube, the main periods reproduce correctly the number of rotational axis and, for the cases of two rotation axis, the relation of the rotation periods. The periods of the Fourier decomposition itself were – not unexpectedly – found to be far off when the simulated observation interval was only of the order of the period itself, and close to the simulated period up to a symmetry factor for analysis of longer observation intervals. The analysis of the simulated light curves indicated that the Fourier analysis in the detection of the main rotation periods is largely independent of the phase angle as long as – as the MLI case seems to indicate – the object is not invisible for large parts of the observation interval.

The Fourier analysis of the real light curves revealed no significant period for the spin-stabilized satellite which only rotates around its symmetry axis. For the upper stage and the Gorizont satellite, two to three rotation periods could be detected, which seem to be stable over a couple of days and seem to be independent of the phase angle under which the objects are observed. Extremely small periods, of the order of a few seconds only, have been detected.

A pattern recognition algorithm was developed and tested on the simulated light curves. In all real light curves, patterns could be detected. The patterns are not identical for different light curves of the same object, but are clearly different for the two different objects compared to each other in the cases regarded here. The size of pattern that could be found is of the order of the rotation periods detected in the Fourier analysis.

## VIII. Acknowledgments

Many thanks go to Martin Ploner, the technical head of the Zimmerwald Observatory, responsible for the operational software to take light curves with such a good sampling rate and to our observers, who supported me in gaining light curves: Marcel Prohaska, Johannes Herzog, Alexander Scartazzini, Stefan Funariu, Alexander Läderach, Simon Willi. The work was supported by the Swiss National Science Foundation through grants 200020-109527 and 200020-122070.